Proc. Estonian Acad. Sci. Engng., 1998, **4**, 1, 3–17
https://doi.org/10.3176/eng.1998.1.01

POSSIBILITIES OF EVALUATION OF POWDER PARTICLE GRANULOMETRY AND MORPHOLOGY BY IMAGE ANALYSIS

Priit KULU[a], Aleksei TÜMANOK[a], Valdek MIKLI[b], Helmo KÄERDI[c], Ivan KOHÚTEK[d], and Michal BESTERCI[d]

[a] Department of Materials Technology, Tallinn Technical University, Ehitajate tee 5, EE-0026 Tallinn, Estonia; e-mail: jakob@edu.ttu.ee
[b] Centre for Materials Research, Tallinn Technical University, Ehitajate tee 5, EE-0026 Tallinn, Estonia; e-mail: miku@edu.ttu.ee
[c] Department of Mathematics, Estonian National Defence and Public Service Academy, Kase tee 5, EE-0020 Tallinn, Estonia
[d] Institute of Materials Research of the Slovak Academy of Sciences, Watsonova 47, 043 53 Košice, Slovak Republic

Received 9 September 1997, in revised form 7 January 1998

Abstract. Particle granulometry and morphology determine the main technological properties of powders and the properties of powder materials, i.e., those of the final product. Different methods, such as sieving and image analysis, are available for powder granulometry and morphology evaluation. In the granulometry studies by granulometric analysis, the modified Rosin–Rammler distribution function and the method were used. The morphology of different powders (atomized and ground) was evaluated by two methods of image analysis. The powder granulometry is adequately described by the modified Rosin–Rammler distribution function. The comparison of the two methods of image analysis showed that the Image Processing System Videolab is more suitable for particle size evaluation, but by the Standard DIPS method, the morphology can be described in detail.

Key words: powder, granulometry, morphology, image analysis.

1. INTRODUCTION

The mono- or polycomposite powders, produced by various methods, are the basic elements in powder metallurgy. These methods include milling, reduction of oxides, carbonization methods, atomization by various media (water, gas and plasma) and methods of evaporation and condensation. Each of these methods

produces a powder of a certain quality, particle size, and morphology. The structural parameters of a compact body made from the powder and its properties depend on these parameters. In addition to size, morphology is a very important parameter. It is evaluated by a description (e.g., spherical, angular, dendritic, dish-shaped, and acircular) or quasi-quantitatively, e.g., by means of a geometrical shape factor.

The granulometry of powders can be determined by different methods (sieving analysis and image analysis), but the question is – how adequately they describe the powder granulometry. Owing to the information of their adequacy, it is possible to control the processes of powder production, first producing powders with the determined properties to choose the optimal condition of grinding (such as direct, separative, selective).

Recent developments in image analysis facilitate the quantitative description of morphology. The aim of this study was to develop an improved method for morphology description.

2. EXPERIMENTAL

Our analysis was carried out on three morphologically different powders, namely superbronze powder (marked *A*) produced by atomizing, brass powder (*B*), and hard metal powder (*C*) produced by disintegration. The geometrical shape of the powders under study is illustrated in Fig. 1.

2.1. Granulometry of the powder

To describe the granulometry of powders produced by collision milling, we used two methods: granulometric analysis and image analysis. To study the granulometry of powders by the granulometric analysis, the modified Rosin–Rammler distribution function and method were used [1].

The granulometry of powders was described by Rosin–Rammler in the logarithmic size of particles x

$$x = \log_k \frac{X_0}{X}, \tag{1}$$

where X and X_0 are the natural and the upper limit of possible size of particles, and k is the coefficient (ratio) of the sieve system used in experiments ($k = 2$, 2^5, 2^{25}, in our experiments $k = 2$).

The modified Rosin–Rammler distribution function was applied in the differential form f_m

$$f_m(x, x_0, m, n) = \frac{n-1}{m} Z^{n-1} \exp\left(-\frac{n-1}{m} Z^n\right), \tag{2}$$

and in the integral one F_m

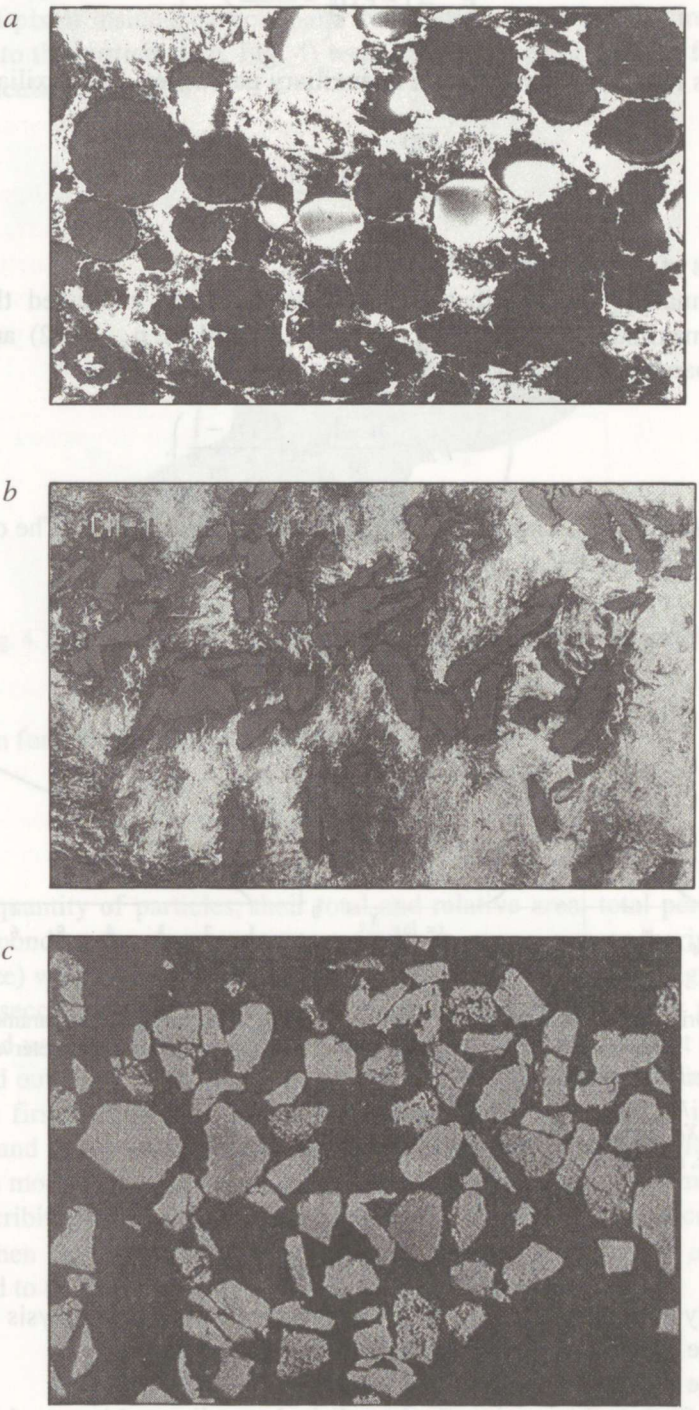

Fig. 1. Original images of powders A (a), B (b), and C (c).

$$F_m = 1 - \exp\left(-\frac{n-1}{n} Z^n\right), \tag{3}$$

where m is mode of distribution, n is auxiliary parameter, and auxiliary variable Z equals

$$Z = \frac{x - x_0}{m}. \tag{4}$$

Parameters of distribution are shown in Fig. 2.

Unfortunately, the distribution function cannot be expressed through the value of maximum probability p_m directly. Instead of p_m, in (2) and (3), the auxiliary parameter n is used. Parameter p_m is expressed by

$$p_m = \frac{n-1}{m} \exp\left(-\frac{n-1}{m}\right). \tag{5}$$

The expression $m \cdot p_m$, shown in Fig. 3, is the function of n only. The dependence of p_m on n is nearly linear.

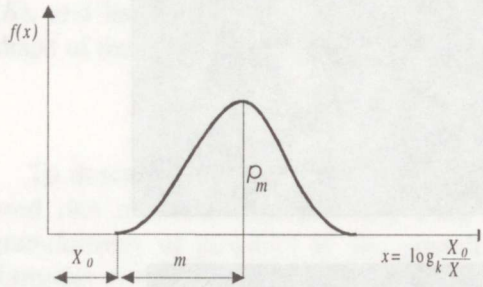

Fig. 2. The principal parameters of the used distribution function; $X_0 + m$ – the logarithmic size of particle with maximum probability, p_m – value of maximum probability, X_0 – upper limit of the largest particle, m – mode of distribution.

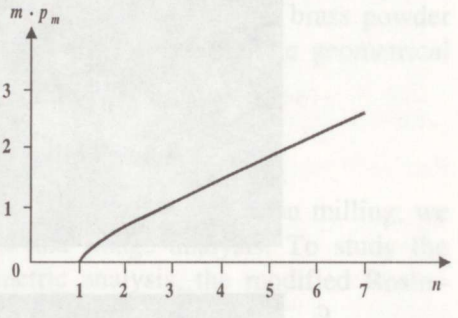

Fig. 3. Dependence of parameter p_m on auxiliary parameter n.

2.2. Morphology of the powder particles

To study the morphology, two different methods of image analysis were used:

1. Image Processing System Videolab (version 2.1) [2]
2. Image Analysis standard DIPS methods (version 4.0) [3].

By the first method, using finely polished metallographic samples, the half tone images were stored by a TV-camera in the computer and were digitized. In

the second step of the morphological analysis, the particle perimeter P_i, area A_i (the area of pixels inside a particle), and diameter d_i (diameter of a circle with an area equal to the particle area, Fig. 4) were measured. After that the form factor K_{fi} was calculated

$$K_{fi} = \frac{4\pi A_i}{P_i^2}. \tag{6}$$

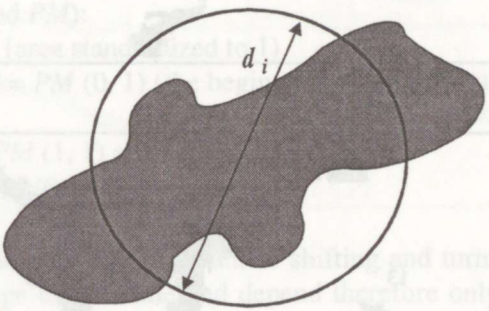

Fig. 4. Morphology study based on the circle with equal perimeter of particle.

Medium form factor K_{fm} was calculated by the formula

$$K_{fm} = \frac{4\pi}{n} \sum_{i=1}^{N} \frac{A_i}{P_i^2}. \tag{7}$$

Next, the quantity of particles, their total and relative area, total perimeter and the corresponding average parameters (average area, average perimeter, and average size) were calculated and shown in size/form distribution diagrams.

By the second method, photographs of structures were stored by means of a scanner and used as an input for an image analyzer. The subsequent processing was carried out by means of the image analyzer DIPS (version 4.0), in which the image was first modified by various filters and transformations to increase its sharpness and to separate the objects studied. The objects studied are shown in Fig. 5. The modified image was then analysed by the standard DIPS methods [3].

By describing powder particle morphology, let G be the geometrical object in a plane. Then the general geometrical moment $M(\mu,\nu)$ (moment of $\mu+\nu$ order) with regard to (x, y) coordinate system axes is defined as follows:

$$M(\mu,\nu) = \iint_G x^{\nu} y^{\mu} dxdy. \tag{8}$$

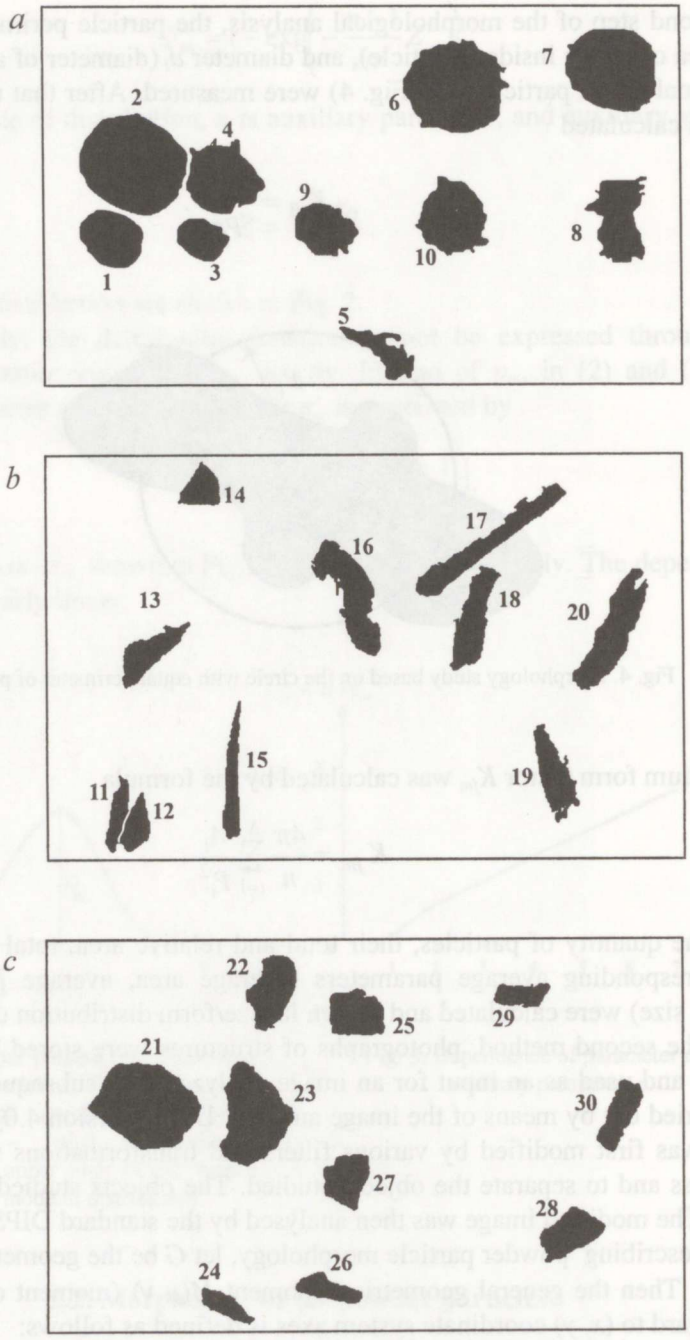

Fig. 5. Particles selected for evaluation from the original images of powders *A* (*a*), *B* (*b*), and *C* (*c*).

While the object is in a plane divided into pixels (squares of area p), the following sum replaces an integral in the calculation of moments:

$$M(\mu,\nu) = \sum_i \sum_j x_i^{\nu} y_j^{\mu} p\,, \tag{9}$$

where x_i, y_j run through the centres of all pixels of the object.

The principal system of coordinates corresponding to the given object is a right-handed rectangular system with the following properties of general geometrical moments, calculated in the selected system of coordinates S (called principal and marked PM):

1. $PM\ (0, 0) = 1$ (area standardized to 1)
2. $PM\ (1, 0) = 0 = PM\ (0, 1)$ (the beginning of the system S is at the centre of gravity)
3. 2nd moment $PM\ (1, 1) = 0$
4. $PM\ (2, 0) \Downarrow PM\ (0, 2)$
5. $PM\ (3, 0) \Downarrow 0$

The principal moments are invariant to shifting and turning of the object as well as to the change of the scale and depend therefore only on its geometrical shape. The moments can be used to calculate additional more or less descriptive characteristics. Two of them are the half-axes a and b of the Legendre's ellipse (Fig. 6). Legendre's ellipse is an ellipse which, up to the 2nd order, has the same moments as the object. Its half-axes can be described as follows:

$$a = 2\sqrt{PM\,(2, 0)}, \qquad b = 2\sqrt{PM\,(0, 2)}. \tag{10}$$

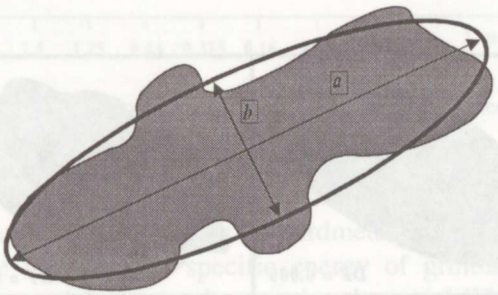

Fig. 6. Morphology study based on the ellipse with an equal area of particle.

Elongation EL is defined by the relationship

$$EL = \log_2 \frac{a}{b}.$$

The elongation for a circle is $EL = 0$, for an ellipse with the ratio of axes 1:2 $EL = 1$, and it grows for the ellipses with bigger ratios of major and secondary axes (Fig. 7).

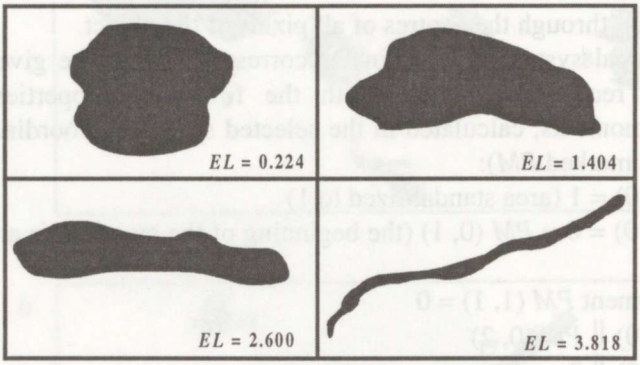

Fig. 7. Elongations for objects with different shapes.

Dispersion DP is defined by the relationship

$$DP = \log_2(\pi ab).$$

This characteristic shows the range of difference between the objects and an ellipse. For an ellipse $DP = 0$, and the higher the "fringing", the higher the DP is (Fig. 8).

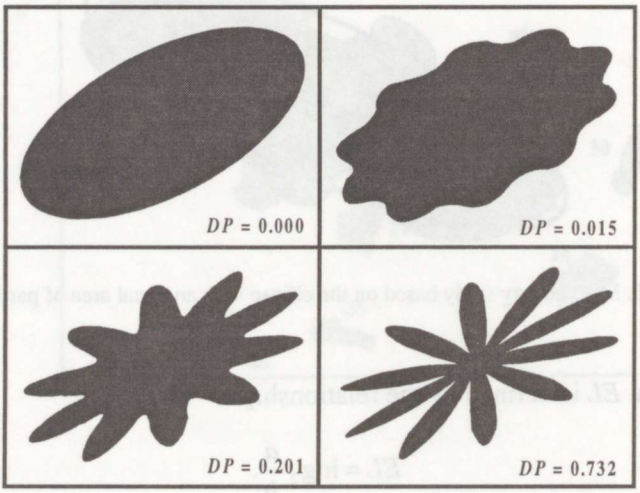

Fig. 8. Dispersions for objects with different shapes.

3. RESULTS

3.1. Granulometry of the powder

The granulometry of the powder produced by collision milling described by the Rosin–Rammler distribution function depends on the specific energy of grinding E as demonstrated in Figs. 9 and 10.

As shown in Fig. 9 and confirmed by the rule of milling of ductile materials [4], considerable refining takes place after first grinding. During the following grindings, the material is not further refined. To achieve a finer fraction, over 10–20 cycles are necessary in a multi-stage grinding. As a result, the fatigue process will take place, and the fine fraction is produced.

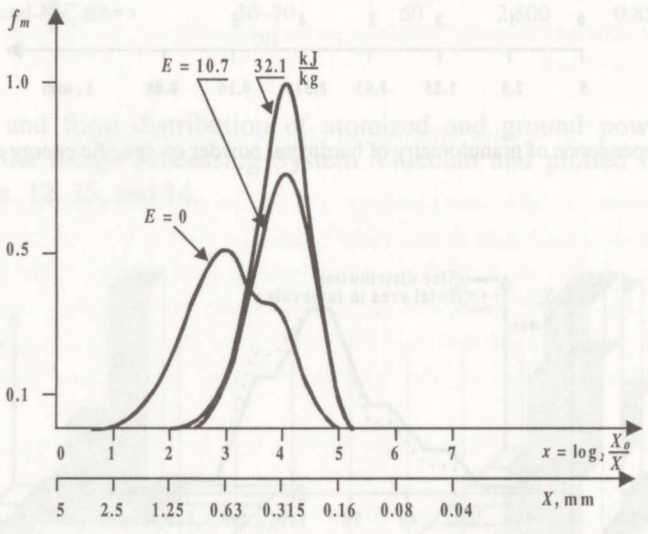

Fig. 9. Dependence of granulometry of brass powder on specific energy of grinding.

On the basis of the study of grindability and fracture mechanism of brittle materials [4], we can state that milling of hardmetals takes place as a result of direct fracture. The influence of specific energy of grinding (multiplicity of grinding) by initial material on granulometry is substantial (Fig. 10).

The output of Image Processing System Videolab is the diagrams describing the distribution of particles as dependent on their size, areas, and form factor (Fig. 11).

Some results of the granulometry study of powders, based on these diagrams, are illustrated in the table. The particles produced by atomizing (powder *A*) basically have a form approaching the spherical one ($K_f = 0.89$–0.95), the particles produced by disintegrator milling (powder *B*) have mainly an isometric form – powder *B* with $K_f = 0.63$–0.65, powder *C* with $K_f = 0.72$–0.85.

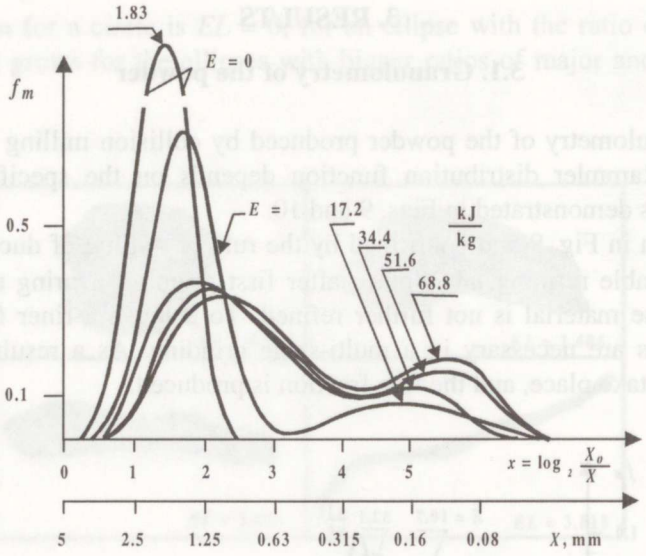

Fig. 10. Dependence of granulometry of hardmetal powder on specific energy of grinding.

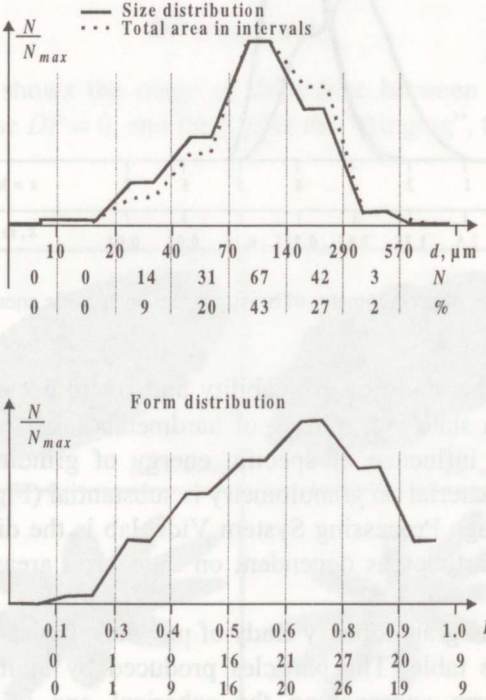

Fig. 11. Diagrams of size and form distribution of particles, where N and N_{max} are the number and the maximal number of particles.

The main characteristics of powders

Material	Granulometry			Form factor K_f	
	Main fraction, μm and %	d_m, μm	A_m, μm^2	Main fraction	Medium fraction
Powder *A* Atomized bronze BRONZTEC +40 –100 μm	50–90 90	75	4 400	0.95	0.89
Powder *B* Ground brass CuZn40Pb +160 –315 μm	60–270 85	140	15 000	0.65	0.63
Powder *C* Ground hardmetal WC-Co –315 μm	30–70 70	60	2 800	0.85	0.72

The size and form distribution of atomized and ground powder particles obtained by the Image Processing System Videolab and plotted in graphs are shown in Figs. 12, 13, and 14.

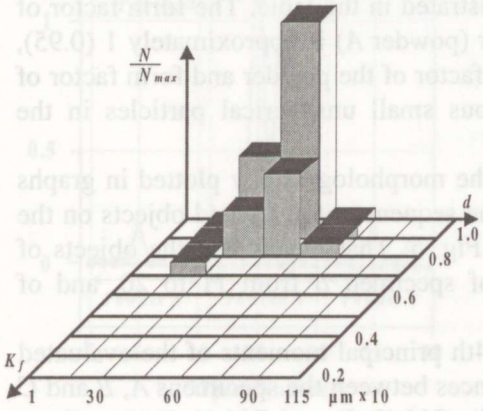

Fig. 12. Size and form distribution of super-bronze particles of bronze powder (powder *A*).

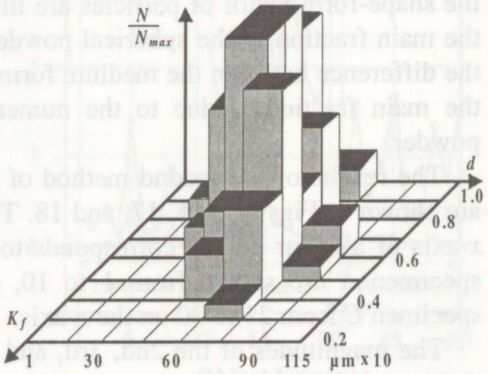

Fig. 13. Size and form distribution of particles of brass powder (powder *B*).

By comparing the results of the granulometry study of the powder produced by milling (powders *B* and *C*), differences in the results of sieving and image analysis were observed. The Rosin–Rammler distribution curve (Figs. 9 and 10) shows that the main fraction of brass and hardmetals powders is 63–160 and 80–160 μm, respectively. As a result of image analysis, we have 60–270 and 30–70 μm, respectively (see table).

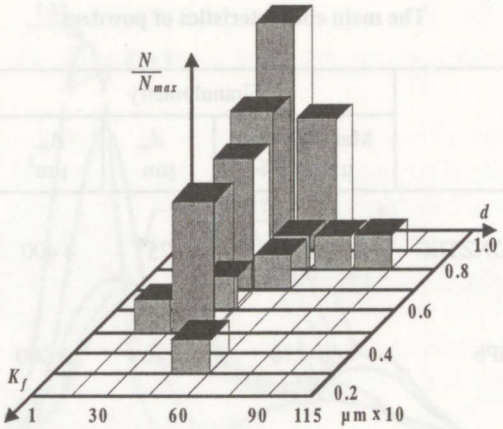

Fig. 14. Size and form distribution of particles of hardmetal powder (powder *C*).

3.2. Morphology of the powder particles

Some results of the morphology study of the powder particles by the micropolishes are shown in Figs. 12, 13, and 14, and the main characteristics of the shape-form factor of particles are illustrated in the table. The form factor of the main fraction of the spherical powder (powder *A*) is approximately 1 (0.95), the difference between the medium form factor of the powder and form factor of the main fraction is due to the numerous small unspherical particles in the powder.

The results of the second method of the morphology study plotted in graphs are shown in Figs. 15, 16, 17, and 18. The sequence of evaluated objects on the *x*-axis of all four graphs corresponds to Fig. 5. That means that the objects of specimen *A* are shown from 1 to 10, of specimen *B* from 11 to 20, and of specimen *C* from 21 to 30 on the *x*-axis.

The magnitudes of the 2nd, 3rd, and 4th principal moments of the evaluated elements indicate that the greatest differences between the specimens *A*, *B* and *C* were observed for the moments *PM* (2, 0), *PM* (3, 0) and *PM* (4, 0), i.e., those which correspond to the distribution around the *y*-axis, while the mixed moments were approximately the same for all the specimens evaluated. The values of elongation *EL* show more pronounced differences (Fig. 18) and suggest that the evaluated objects of specimens *A* and *C* were less elongated than the objects of specimen *B* (also shown in Fig. 5). The values of dispersion *DP* were approximately the same in both specimens, which could be expected with regard to the relative smoothness of configurations (approx. convex). Object No 5 (specimen *A*, Fig. 5) was selected intentionally as an object differing by its shape from all others. This was reflected in all graphical relationships.

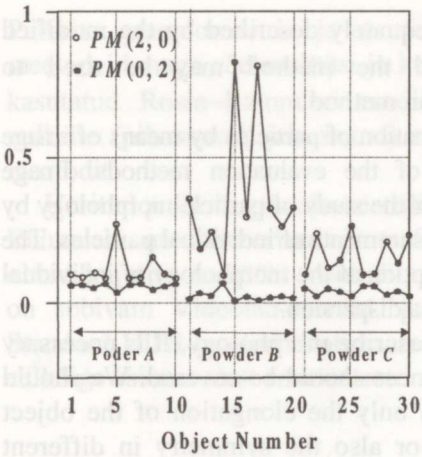

Fig. 15. 2nd principal moments of evaluated particles.

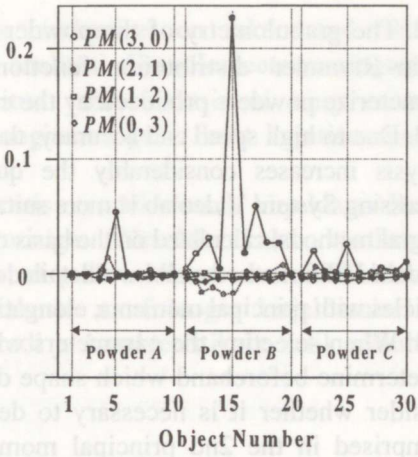

Fig. 16. 3rd principal moments of evaluated particles.

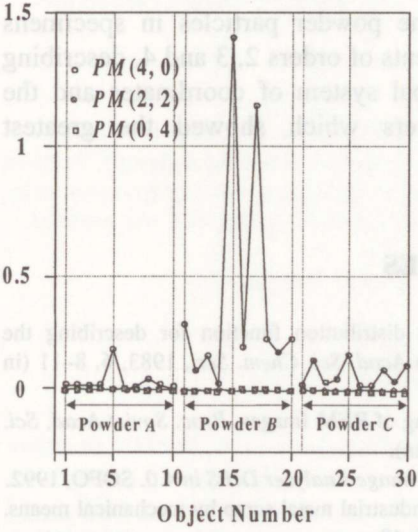

Fig. 17. 4th principal moments of evaluated particles.

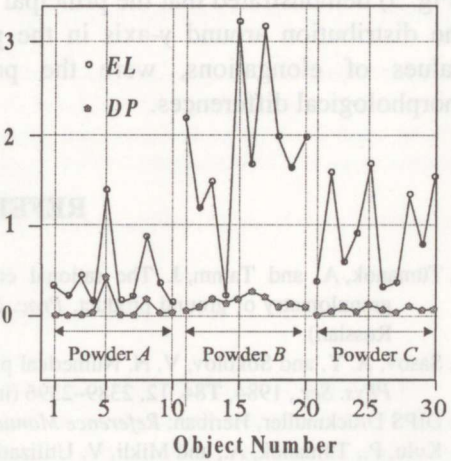

Fig. 18. Elongation and dispersion of evaluated particles.

4. CONCLUSIONS

The results of our study can be summarized as follows.

1. Evaluation of the powder granulometry by means of sieving analysis and image analysis depends on the distribution functions and on the image processing system.

2. The granulometry of the powder is adequately described by the modified Rosin–Rammler distribution function, and the method may be used to characterize powders produced by the collision method.

3. Due to high speed and accuracy, the evaluation of particles by means of image analysis increases considerably the quality of the evaluation methods. Image Processing System Videolab is more suitable for the study of particle morphology by integral methods, calculated on the basis of measurements of individual particles. The standard DIPS method enables a detailed description of the morphology of individual particles with principal moments, elongation, and dispersion.

4. When selecting the parameters which describe morphology, it is necessary to determine beforehand which shape differences should be covered. We should consider whether it is necessary to describe only the elongation of the object (comprised in the 2nd principal moments) or also the symmetry in different directions (3rd principal moments), or possibly some other geometrical characteristics. For this reason, it is impossible to recommend a particular characteristic as the best one. The selection of optimum characteristics will always depend on real requirements.

5. The analysis of the morphology of the powder particles in specimens (Fig. 5) demonstrated that the principal moments of orders 2, 3 and 4, describing the distribution around *y*-axis in the principal system of coordinates and the values of elongations, were the parameters which showed the greatest morphological differences.

REFERENCES

1. Tümanok, A. and Tamm, J. The rational empirical distribution function for describing the granulometry of ground product. *Proc. Siberian Acad. Sci. Chem. Ser.*, 1983, **6**, 8–11 (in Russian).
2. Sasov, A. Y. and Sokolov, V. N. Numerical processing of REM Images. *Proc. Soviet Acad. Sci. Phys. Ser.*, 1984, **T84**, 12, 2389–2396 (in Russian).
3. DIPS Drückmüller, Heriban: *Reference Manual to an Image Analyzer DIPS in 4.0*. SOFO, 1992.
4. Kulu, P., Tümanok, A., and Mikli, V. Utilization of industrial metal scrap by mechanical means. *Proc. Estonian Acad. Sci. Engng.*, 1996, **2**, 1, 36–48.

PULBRIOSAKESTE GRANULOMEETRIA JA MORFOLOOGIA HINDAMISE VÕIMALUSED KUJUTISE ANALÜÜSI TEEL

Priit KULU, Aleksei TÜMANOK, Valdek MIKLI, Helmo KÄERDI, Ivan KOHÚTEK ja Michal BESTERCI

Pulbriosakeste granulomeetria ja morfoloogia määravad pulbrite põhilised tehnoloogilised omadused ja lõpp-produkti – pulbermaterjalide omadused.

Pulbrite granulomeetria ja morfoloogia hindamisel on rakendatud mitmeid meetodeid, nagu sõelanalüüsi ja kujutise analüüsi. Granulomeetriauuringutes on kasutatud Rosin–Rammleri modifitseeritud jaotusfunktsiooni ning erinevate pulbrite (pihustatud, jahvatatud) morfoloogiauuringutes kaht kujutise analüüsi meetodit.

Uuritud pulbrite granulomeetriline koostis on adekvaatselt kirjeldatav Rosin–Rammleri modifitseeritud jaotusfunktsiooniga. Võrreldes kahte vaatluse all olnud kujutise analüüsi meetodit, selgub, et pulbriosakeste suuruse hindamisel on sobivam Videolab-meetod, pulbriosakeste morfoloogia kirjeldamisel aga Standard DIPS-meetod. Optimaalse meetodi ja karakteristikute valik sõltub aga eelkõige esitatavatest erinõuetest.